International Journal for Housing Science and Its Applications
Publish August 10, 2025. Volume 46, Issue 4 Pages 5813-5826

https://doi.org/10.70517/ijhsa464419

Low Voltage Ride-Through Control Method of Photovoltaic Grid-connected Power Generation System in View of Intelligent Wireless Sensor

Zheng Na[1,*], Dantian Zhong[1], Xuejie Wang[1], Zhichao Wen[2], Yang You[2] and Yixuan Wang[1]
[1] School of Electric Power, Shenyang Institute of Technology, Shenyang, Liaoning, 110000, China
[2] Panjin Power Supply Company, State Grid Liaoning Electric Power Co., Ltd., Panjin, Liaoning, 124000, China
Corresponding authors: (e-mail: 76352648@163.com).

Abstract This article proposes a low-voltage ride through control (LVRT) strategy based on reactive current support to address the voltage instability problem in smart sensor photovoltaic grid connected power generation. By preventing overcurrent faults in photovoltaic (PV) and increasing the grid voltage to a certain extent. Restore the voltage of the grid connection point to achieve LVRT. The simulation results show that when the voltage drops by 60%, the voltage at the grid connection point without a control strategy increases by 2 times. After adopting this control strategy, the voltage at the grid connection point increased from 0.314 to around 0.38. When the voltage drops by 30%, the active current is the rated current, and the reactive current increases by 0.45. The voltage at the grid connection point increased from 0.68 to 0.72. Experimental results have shown that this strategy can deliver a certain amount of reactive power to the power grid, causing the voltage at the grid connection point to rise to a certain extent, thereby maintaining the PV station on the grid during power grid faults.

Index Terms PV Grid-Connected, Low Voltage Ride Through, Inverter Control Strategy, Reactive Current Support

I. Introduction

The need for energy is rising daily in tandem with the world economy's fast expansion. Traditional energy resources such as petroleum and coal are extremely limited. Coupled with the substantial increase in their prices and the rising cost of power generation, the transformation of traditional models has become inevitable. Solar energy has become the best choice, not only rich in resources, but also conducive to environmental protection. So the PV has been developed rapidly. However, the motor capacity of the photovoltaic system is extremely limited and easily affected by external factors. It was only used as a load on the grid before it was merged with the power generation system. Therefore, it is usually connected in parallel to the distribution feeder of the secondary substation when it is connected in parallel with the power company. When the PV supply is connected with the electricity generation system, it can interfere with the normal functionality of the production system.When there are abnormalities in the voltage at the point of application of the PV supply to the generation system caused by external factors, the system will automatically disconnect from the PV, to prevent unstable voltage from bringing more serious consequences to the system. But this mode is only effective for PV plants with small power generation capacity. If a solar power station with a large power generation capacity runs outside the system, it will not only fail to make the system operate normally, but it will also cause greater losses. The most serious consequence is the collapse of the entire system.

In response, it is necessary to address the issue of losses in the generation system due to voltage instability.This paper studies the use of low voltage rerouting control technology as a means of combating this problem. This strategy is to allow the PV station to disconnect from the power generation system only when the system cannot resume normal operation within specified amounts of time. In this way, when short-term failures are eliminated and the system can resume normal operation,The PV plant can continue to operate with no compromise on generating system stability. In the meantime, the PV plant can contribute to the generation system by assisting in voltage stabilisation by offering the generating system the support of passive power.

At present, there are a lot of discussions on the solution to the problem of PV grid-connected power generation system failure. Haddadi A M studied an individual three-phase cold source inversion (CSI) for a grid connected photovoltaic (PVGC) system, proposed an optimal predictive grid current control (DPOC) strategy, and proposed an anti-disturbance greatest peak potential tracking (PR-MPPT) arrangement for the CSI PVGC system.By conducting experiments on the proposed method, it was demonstrated that the CSI PVGC system has the characteristics of simple circuit, good stability, high dynamic response and MPPT function, and verifies its feasibility

[1].Madeti S R believes that surveillance systems are crucial to keeping the optimal implementation of PV systems, he proposed a new fault detection technique for analyzing the anomalies noticed in the faulty PV strings and the terminal characteristics of the appropriate arrays, using the differential values of terminal voltages of modules within healthy strings and healthy modules within unhealthy strings to identify malfunctioning modules, this method has the principal advantage of not requiring string current sensors but using the optimal placement of voltage sensors the number of voltage sensors is decreased, the final experimental outcome demonstrates the validity of the suggested fault detection technique [2]. Zaim R proposes an innovative low-cost, non-intrusive as well as disconnected sensing technique to be used in connection with grid-connected PV inverters, which represents an excellent example of an algorithmic solution to the problems related to control of CCMs in a manner similar to the simplicity of boundary and discontinuous conduction modes. The results show that the prototype contains a mains current THD of 1.9%, a power factor of 0.9988, a resting MPPT frequency of more than 99% and a variable efficiency of 98.50%, all consistent with the conditions[3]. Hasanien H M presents an new application of an adaptation control strategy for grid connected PV plants to enhance the under LVRT capability based on the continuous mixed p-number (CMPN) method. His simulations using PSCAD/EMTDC simulator have extensively validated the effectiveness of the adaptive control strategy[4]. Hassan Z believes that grid-connected PV can greatly reduce the world's dependence on traditional energy sources. He outlined the inverter topology, including power processing stages, transformers and transformerless inverters, multi-level inverters, flexible and tough-switching, two-way and mixing inverters. He discussed and checked the current injection technology with LVRT control strategy, and compared the advantages and disadvantages of the control scheme [5]. In his overview and comparison of various FRT capability augmentation techniques for electrical grids under fault conditions, Al-Shetwi A. Q. separates these techniques into two main groups based on control type and connectivity settings: external device-based techniques and modified controller-based techniques. He then goes into some detail about the advantages and disadvantages of each technique, comparing them in terms of grid regulation compliance, controller sophistication, and He also compares these approaches in terms of controller sophistication, grid code compliance, and economics, and he comes to the conclusion that the modified inverter controller (MIC) is the most effective way to achieve FRT capability among the other forms of regulation [6]. Jaalam N proposes an active and reactive power control strategy for a single-stage, three-phase grid-connected PV system to improve LVRT.The dynamic behaviour of the system is investigated by considering various scenarios in various locations within the operation of a multi-distributed power supply, for instance different illumination levels, local load disconnections and short circuits. The findings verify that the grid-connected PV system is able to maintain its connection to the grid under state and instantaneous conditions while not infringing grid code demands [7]. Regarding the problem of PV grid-connected voltage instability, most scholars have conducted research from the aspects of inverter topology and rotor protection. This kind of research technology is complicated to operate, and the cost is relatively high.

In the case of a PV grid failure, the LVRT control method proposed in this research supports the reactive power of the grid-connected network voltage to meet varying depths of power dips and accomplish varying amounts of reactive power compensation. The parameters derived from the simulation study using this technique are applicable to the system with excellent accuracy. When the grid fails, this technique can provide LVRT and reduce the strain on the inverter to make up for the reactive voltage. It enhances solar grid-connected systems' stability and power supply dependability. And compared with the first two technical strategies, it is easier to operate and the cost is more reasonable, which is conducive to large-scale implementation and application.

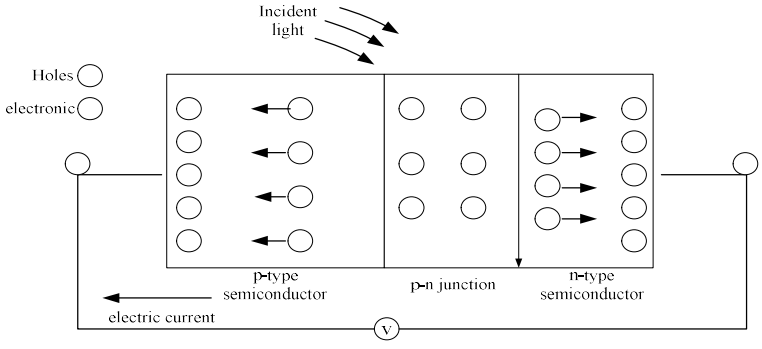

Figure 1: p-n junction PV principle

II. LVRT Control Method of Photovoltaic Grid-connected Power Generation System

II. A. Relevant Basis for Photovoltaic Grid-connected Power Generation

II. A. 1) The Working Principle and Characteristics of PV Cells

By using the photoelectric or photochemical effects, PV cells may directly transform the light energy of sunshine into electrical energy. New hole-electron pairs are created when sunlight strikes the semiconductor p-n junction [8]. The p-n junction's electric field causes electrons to go from the p zone to the n zone and holes to move from the n zone to the p zone. A current is created after the circuit is linked, as seen in Figure 1:

The formula of load current I_L is:

$$I_L = I_S - I_{ks} - \frac{U_L + I_L R_S}{R_{sh}} \tag{1}$$

Among them,

$$I_{gs} = I_{dl}\left(\frac{S}{1000}\right) + W_T\left(T - T_{ab}\right) \tag{2}$$

$$I_{ks} = I_{sat}\left(e^{\frac{q(U_L + I_L R_s)}{AKT}} - 1\right) \tag{3}$$

$$I_{sat} = I_{rc}\left(\frac{T}{T_{ab}}\right)^3 e^{\left[\frac{qB_{ge}}{AK}\left(\frac{1}{T_{ab}} - \frac{1}{T}\right)\right]} \tag{4}$$

A large number of ground PV systems use silicon solar cells based on silicon, which are classified as single-crystalline silicon, multiple-crystalline silicon and non-crystalline silicon solar cells [9]. The formula for calculating the output current of this battery under ideal conditions is [10]:

$$I_L = I_{gs} - I_{ks}\left(e^{\frac{qU_L}{AKT}} - 1\right) \tag{5}$$

The output voltage of PV cell is expressed as [11]:

$$U_L = \frac{AKT}{q}\ln\left(\frac{I_{gs} - I_L}{I_{ks}} + 1\right) \tag{6}$$

The formula variable indications are shown in Table 1:

Table 1: Formula variable meaning

variable name	meaning	illustrate
I_{gs}	Photocurrent	variable
I_{ks}	Diffusion current	variable
I_{dl}	Short circuit current	variable
S	Sunlight intensity	variable
W_T	Temperature Coefficient	constant
T	Battery temperature	variable
T_{ab}	Absolute temperature	237K
A	Ideal constant of diode	Unknown constant
K	Boltzmann constant	$1.38\times10^{-23}\,J/K$
q	Electron charge	$1.6\times10^{-19}\,C$
I_{rc}	Diode reverse current	Unknown constant

B_{ge}	Band gap energy	1.2eV

According to formula 6, the characteristic curve of PV cell current and power output can be drawn. As shown in Figure 2, U_{oc} is the open circuit voltage of the PV cell, U_{max} is the voltage when the PV cell is working at the maximum power point, I_{max} is the current when the PV cell is working at the maximum power point, and P_{max} is the maximum power of the PV cell.

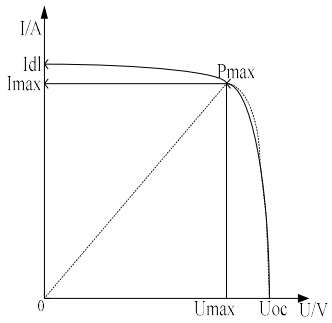

Figure 2: Characteristic curve of PV battery current and power outpute

The dotted line represents the output power characteristic curve of the PV array after the power P is reduced in a certain proportion. The output power is equal to the load current multiplied by the output voltage, which is expressed as [12]:

$$P = I_L U_L \tag{7}$$

It can be seen from the characteristic curve that the rectangular area enclosed by the U value and I value and the horizontal and vertical coordinates at any point on the curve is the output power of the PV cell [13]. In the initial period, the I value of the PV cell is I_{dl}, at this time the U value is zero, and the output power P is also zero. When the value of $U < U_{max}$, the value of I decreases slightly with the increase of the value of U, and the output power P increases with the increase of the value of U at this time; when it reaches U_{max}, the value of P is the maximum at this time. When the value of $U > U_{max}$, the value of I will decrease greatly with the increase of the value of U, and the value of P will also decrease greatly, until the value of I and P are both zero [14]. So in addition to the greatest possible power delivery from the PV cells, it is necessary to observe and control the P_{max} point in real time.

According to the characteristics of PV cell $I-U$, when $I_{dl} = U_{oc}$, P reaches the maximum value, and the photoelectric conversion efficiency reaches the maximum. The fill factor is an influential component in the evaluation of the efficiency of a PV cell. The greater its diameter, the more the output characteristics of the solar cell tend to be rectangular and the better the photoelectric conversion performance. It can be expressed as:

$$FF = \frac{I_{max} U_{max}}{I_{dl} U_{oc}} \tag{8}$$

So [15],

$$P_{max} = I_{dl} U_{oc} FF \tag{9}$$

The characteristic curve of PV cell current and power output will change with the influence of the external environment temperature, as shown in Figure 3:

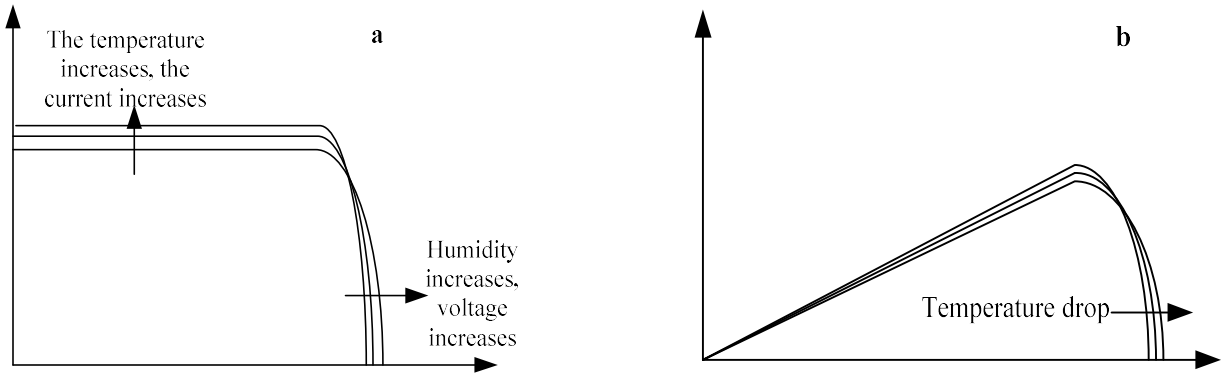

(a) shows the output current characteristics of the PV cell with temperature

(b) shows the the output power characteristics of the PV cell with temperature

Figure 3: Characteristic curve of PV cell current and power output

When the temperature increases, the no-load voltage value shows a decreasing trend, while the short-circuit current changes relatively smoothly. For every degree of temperature increase, one third of efficiency is lost [16]. The output power is inversely proportional to the temperature of the PV cell, which is the negative temperature coefficient that people often say. PV cells are greatly affected by external factors, and they are unstable. To achieve high-efficiency photoelectric conversion, the impact of external factors on PV cells must be considered. It needs to study the characteristic curve of PV cells, track and observe the maximum power point in real time, and realize the maximum utility of PV cells on PV grid-connected systems [17].

II. A. 2) Photovoltaic Grid-connected Technology

The electrical energy output by PV cells cannot be directly incorporated into the grid system. Because the electrical energy it outputs is direct current, it needs to be inverted into alternating current, and then the voltage of the alternating current is raised to the same voltage as the grid system before it can be combined. This is the most important step of PV grid connection, which needs to be operated by an inverter. The excellent performance of the inverter largely determines the success or failure of PV grid connection [18]. The inverter has multiple functions such as LVRT and islanding detection. At the same time, the output performance of the inverter is directly related to the power quality, which has a direct impact on the distribution network. To achieve the maximum output, the inverter needs to be controlled. Different strategies will lead to different output quality of the inverter, and even affect the real-time observation and tracking of PV system points and the level of photoelectric conversion efficiency [19].

Real-time tracking of point P_{max} can be carried out by using the characteristics of the PV system, that is, by using the relationship between the rate of change of conductance and the conductance. When the PV system is operating at point P_{max}, the I of its P - U characteristic curve remains unchanged. That is, the voltage change rate of the P to U wire is 0, and the formula [20] can be obtained from this:

$$\left.\frac{dP}{dU}\right|_{P=P_{max}} = 0 \tag{10}$$

The admittance change rate can be derived from formula 10 [21]:

$$\frac{dI}{dU} = -\frac{I}{U} \tag{11}$$

It can be seen from formula 11 that when the PV system runs to point P_{max}, the rate of change of the admittance is equal to the opposite of the system admittance. Therefore, during the operation of the PV system, whether it is a load change or a problem of the PV system itself, the admittance change rate and admittance calculation and real-time monitoring can be used to verify whether the system is operating at its P_{max} point. Then according to the

I value and U value obtained by real-time monitoring, the corresponding adjustment is made so that the two meet the relationship of formula 11, so that the control of the P_{max} point is realized.

II. B.LVRT Control Technology

II. B. 1) Technical Requirements for LVRT Control

The grid-connected inverter's control system must also adhere to the pertinent grid-connected regulations. The solar output can be linked to the public grid even if the voltage, frequency, and phase differences between it and the grid are all within the permitted range. In other words, as seen in Figure 4, a PV grid connection must satisfy the technical specifications of LVRT.

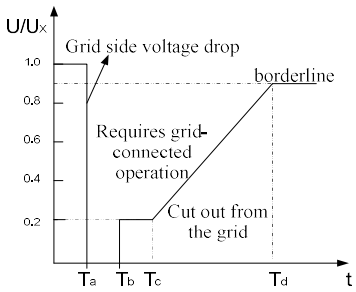

Figure 4: LVRT technical requirements

In Figure 4, U is defined as the actual grid-side pressure, and U_x is defined as the rated voltage. The voltage of the grid-connected point for normal operation of the PV grid-connected system is at least 90% of U_x. The depth of the grid-side voltage drop varies with time. If it is higher than the threshold line, the PV system must remain connected to the grid. The PV system the threshold line must be disconnected from the grid. The actual conditions of each PV system determine the allowable operating time at different descent depths, as shown in Table 2:

Table 2: Allowable running time under different descent depth

Voltage drop degree	Allowable running time
Down 80%	$T_a - T_c$
Down 10%	$T_a - T_d$
Zero drop	$T_a - T_b$

According to the requirements of LVRT technical standards, the corresponding LVRT control strategy of PV station can be formulated to fulfil the technical demands of PV system grid-connected.

II. B. 2) The Dynamic Characteristics of the PV Inverter System When the Power Grid Fails

The power balance relationship of the PV inverter system is [22]:

$$P_{yg} = P_z + P_n \tag{12}$$

Among them, P_{yg} is the active power emitted by the PV array composed of multiple sets of PV cells, P_z is the power of the side supporting capacitor, and P_n is the effective power output from the PV converter system towards the grid system. When system is in steady state-operating condition, the DC side voltage of the inverter system remains stable, and P_z does not change, then:

$$P_{yg} = P_n = 3UI \tag{13}$$

When there is a drop in voltage at the PV grid, the inverted array output remains unchanged because the external environmental parameters remain unchanged and the DC side capacitor voltage cannot change suddenly. On the AC bank of the converter, due to the existence of the filter inductance and the limitation of the amplitude of the AC output current, the P_n of the converter system output to the grid is reduced. Therefore, the converter system will have an instantaneous power imbalance, and the excess energy will rush to the DC side supporting capacitor, resulting in an instantaneous increase in the DC side voltage.

$$\left(P_{yg}-P_n\right)\Delta t=P_z\Delta t \tag{14}$$

Assuming that the grid voltage drops to U', and the capacitor voltage changes to U'_c after a sudden change, then:

$$\left(P_{yg}-3U'I\right)\Delta t=\frac{1}{2}C\left(U'^2_c-U^2_c\right) \tag{15}$$

Because of $P_{yg}=3UI$, according to formula 15 we can know [23]:

$$U'_c=\sqrt{\frac{2P_{yg'}\frac{U-U'}{U}\Delta t}{C}+U^2_c} \tag{16}$$

As shown in formula 16 that the greater the voltage drop at the parallel network, the longer the drop lasts, the higher the voltage on the DC side after the sudden change, until the array output power and the converter system output power reach a new balance, the DC side voltage will be stable.

II. B. 3) Analysis of Low Power Crossing Control Policies On the Basis of Reactive Energy Support

PV grid-connected inverter systems generally operate at unit power under normal conditions, and zero circulating variable current as a reference level. When power voltage falls, the outer voltage loop is disconnected and the circulating energy reference current is taken as shown in the formula, then:

$$I_{qref}=K\frac{\Delta U}{U_n}I_N \tag{17}$$

If the current on the AC side is limited to not more than 1.1 time of the rated current, when the voltage drops, that is, $I^2_d+I^2_q\le\left(1.1I_N\right)^2$. When the voltage drops until the PV station can maintain the worst working conditions of grid-connected operation, if the inverter system outputs all reactive currents, then $\Delta U=\left(0.9-0.2\right)U_N=0.7U_N$ can be obtained from Equation 17:

$$0.7KI_N\le1.1I_N \tag{18}$$

So,

$$k\le1.571 \tag{19}$$

When the active current output of the inverter is $I_d=I_N$, the maximum reactive current allowed to be output is [24]:

$$I_q=\sqrt{\left(1.1I_N\right)^2-I^2_N}=0.46I_N \tag{20}$$

At this time, if $K=1.5$ is taken, without reducing I_d, From Equation 17, the maximum depth that the parallel network voltage would be allowed to dip is:

$$\Delta U\approx0.307U_N \tag{21}$$

That is, when the voltage drops below $0.539U_N$, the active current output must be reduced in order to meet the grid-connected current amplitude requirements. At this time, the active current reference value is [25]:

$$I_{dref}=\sqrt{\left(1.1I_N\right)^2-I^2_{qref}} \tag{22}$$

Among them,

$$I_{qref}=1.5\left(0.9-\frac{U}{U_N}\right)I_N \tag{23}$$

When the voltage drops above $0.593U_N$, in order to enable the inverter system to output reactive current as much as possible, the active output current can be fixed as:

$$I_{dref} = I_N \tag{24}$$

$$I_{qref} = 0.46 I_N \tag{25}$$

The idea behind the above control strategy is: When the parallel network voltage dips in the range of $0.2U_N - 0.9U_N$, the control strategy of the PV inverter system is changed to output a certain degree of reactive current. To a certain extent, increase the grid-connected point voltage to achieve LVRT. The flow chart is shown in Figure 5. This LVRT method only changes the control strategy of the inverter system without adding additional hardware equipment, so it can reduce the cost of power generation.

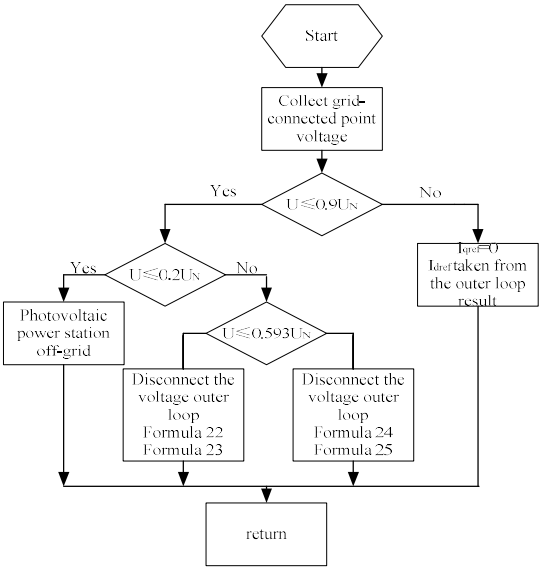

Figure 5: Flow chart of LVRT control strategy based on reactive power support

III. Simulation Analysis of LVRT Control Methods

The simulation is performed on PSCAD (Computer Aided Design of Power System)/EMTDC (Simulation Computing Core), and the LVRT control strategy module is shown in Figure 6. The meanings of the names in the modules are shown in Table 3. The simulation results are analyzed in the following two drop situations.

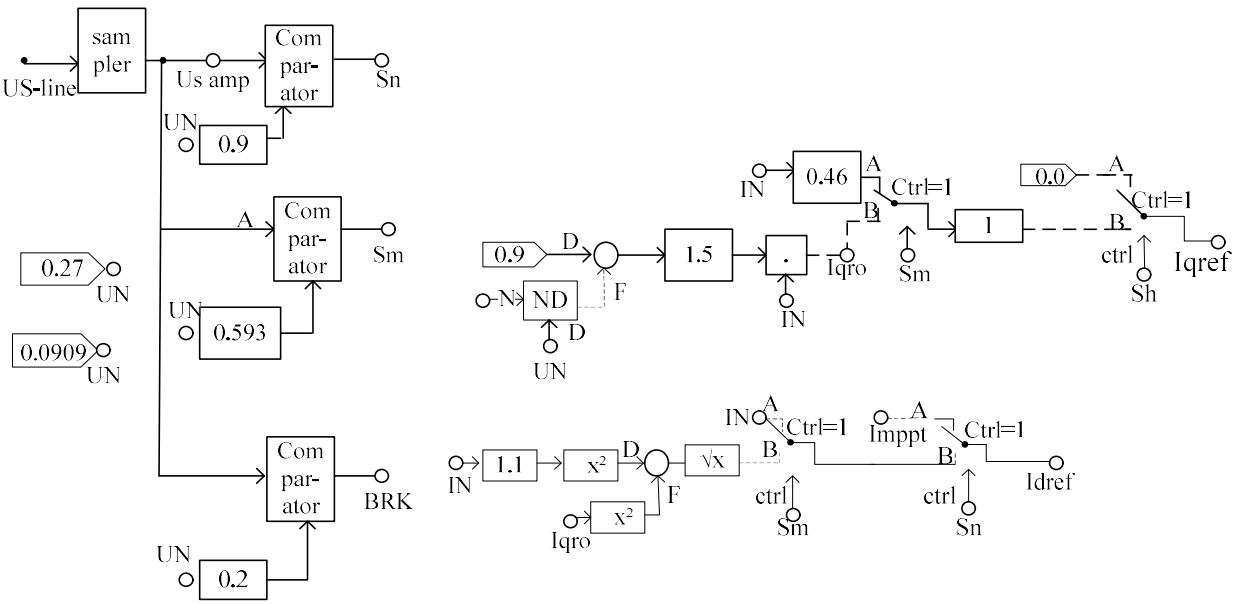

Figure 6: LVRT control strategy simulation module based on reactive current support

Table 3: Name meaning indicator table

appellation	meaning
US-line	Grid-connected voltage amplitude signal
UN	System rated voltage
UI	System rated current
Imppt	Voltage outer loop PI regulator output current signal
BRK	Circuit breaker signal
Idref	System active current reference value
Iqref	System reactive current reference value

(1) The voltage at the grid connection point dropped by 60%.

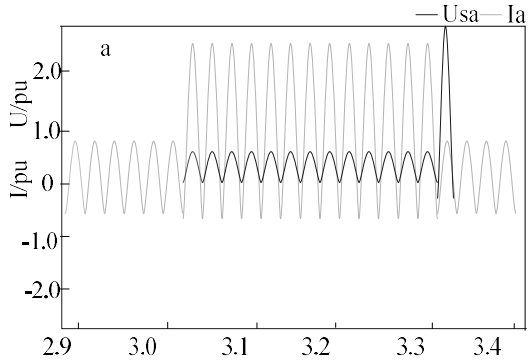

(a) shows an illustration of the precurrent and voltage before the adoption of the strategy

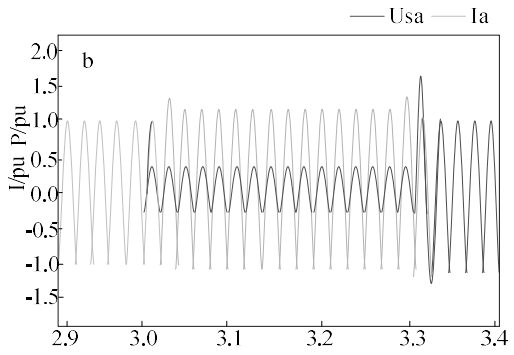

(b) shows an illustration of the precurrent and voltage after the adoption of the strategy

Figure 7: Voltage and current waveforms when the voltage drops 60%

The simulation results show that the parallel current spikes to about twice the rated current when the electrical grid voltage drops by 60 percent. If no measures are taken, the protection device will inevitably be activated to disconnect the PV station from the grid, and thus cannot fulfill the demands of LVRT. The diagram also shows that the parallel voltage and electric phase are the same and the converter is still operating at unit energy consumption. When the LVRT control strategy is not adopted and the grid-connected current is not limited, if a three-phase short-circuit ground fault occurs in the system, the grid-connected point voltage will drop by about 60%. The voltage and current of the grid-connected point are shown in Figure 7a, and the values in the figure are in standard unit values. When the LVRT control strategy is adopted, when the grid voltage drops by 60%, the grid-connected voltage and current are shown in Figure 7b. The diagram shows that the parallel connection current is controlled to within 1.1 time the nominal pressure, and since the active current is already limited, the increase in electricity is the passive component.

Figure 8 is a component diagram of grid-connected current.As shown in Figure 8a, when a decrease in grid electricity occurs before the adoption of the low-voltage crossing technology technique, the increase in grid current is predominantly in the active current, which increases by $1\,\mathrm{pu}$. Therefore, if the grid-connected output of the inverter system is not flowed, it is mainly to control the reference value I_{dref} of the active current in the inner loop of the current. Once the under-voltage crossing control technique has been adopted, as shown in Figure 8b, the active current drops to about $0.82\,\mathrm{pu}$ and the reactive current increases by about $0.75\,\mathrm{pu}$. Due to the injection of reactive current, the inverter no longer operates at unity power factor during the voltage drop.

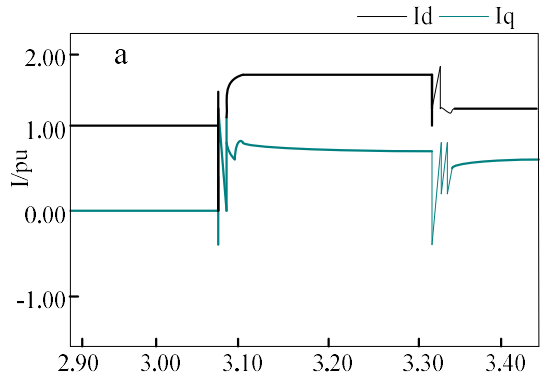

(a) shows the live and passive contributions of the grid-connected current of the converter system at a voltage drop of 60% before the adoption of the strategy

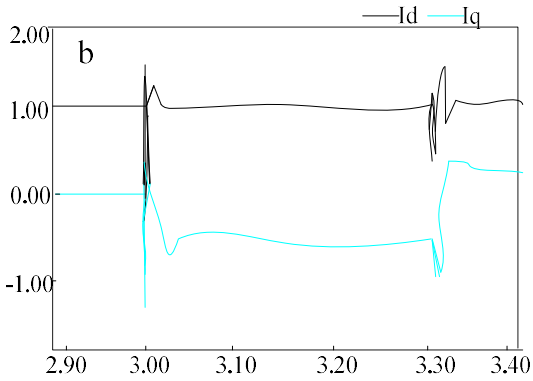

(b) shows the live and passive contributions of the grid-connected current of the converter system at a voltage drop of 60% after the adoption of the strategy

Figure 8: Grid-connected current d and q component diagram

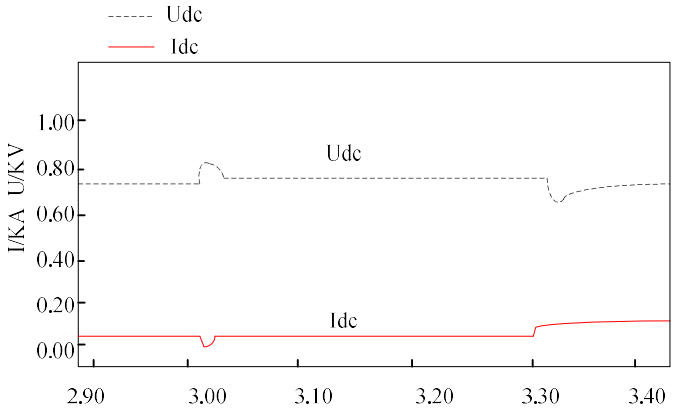

Figure 9: Voltage and current waveforms on the DC side of the inverter system

Figure 9 illustrates the DC-side volume and electric power waveforms of the converter system during a volume drops. In the figure, the DC side voltage increases by about 0.15 pu , and the DC side current decreases by 0.45 pu .

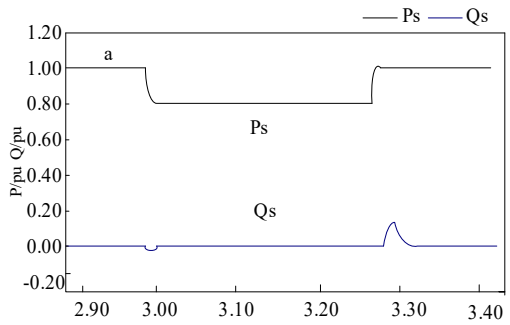

(a) shows that the voltage drops by 60% before the control strategy is adopted, and the system output active and reactive power

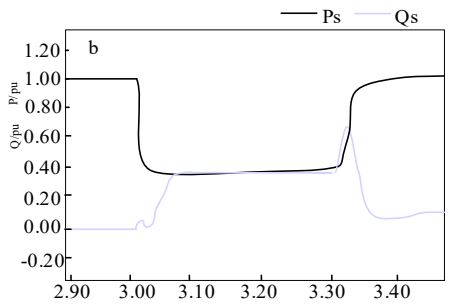

(b) shows that the voltage drops by 60% after the control strategy is adopted, and the system outputs active and reactive power

Figure 10: System output active and reactive power

Figure 10a shows the effective and passive power output of the systems during voltage dips before the low-voltage crossing control measures were adopted, and the effective energy drops to 0.63 pu. The passive power output is zero. Figure 10b shows that the inverter system outputs active power and passive power when the voltage drops by 60% after the system adopts the LVRT control strategy. The active power drops to about 0.316 pu, and the reactive power increases by about 0.296 pu. At this time, the effective energy is reduced by about 0.32 pu compared with before the control strategy is adopted. This is because the effective current is limited.

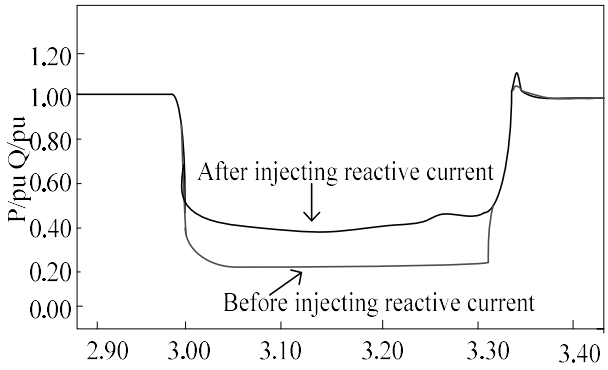

Figure 11: Active power and reactive power after adopting the control strategy

Figure 11 shows the comparison of the grid-connected point volume before and after the system adopts the low-volume crossing control measures. The grid-connected point volume is about 0.314 pu before the reactive current is injected, and it increases to about 0.38 pu after the reactive current is injected. The overall improvement is not very large, which is due to the small capacity of the simulation system.

When the grid voltage drops by more than 59.3%, the result calculated by formula 23 (using the standard unit value) is shown in Table 4:

Table 4: Calculation result when the voltage drops by 59.3%

appellation	Numerical value
Reactive current	0.765
Active current	0.79
Active power	0.308
Reactive power	0.298

The calculation results are consistent with the simulation results, verifying the calibration of the simulation of the low-volume crossing control measures.

(2) The parallel network voltage falls by 30%

After the application of the low-volume crossing control scheme, when the voltage of the parallel network drops by 30%, the parallel network voltage and present are as illustrated in Figure 12. And the grid current is within one point double of the specified level.

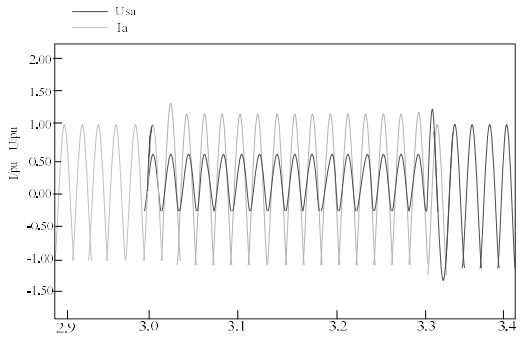

Figure 12: Voltage and current after control strategy

Figure 13 illustrates the effective and passive constituents of the grid-connected current. Since the degree of sag is less than 59.3%, the effective level is qualified to the rated level, and the reactive level increases by 0.45 pu .

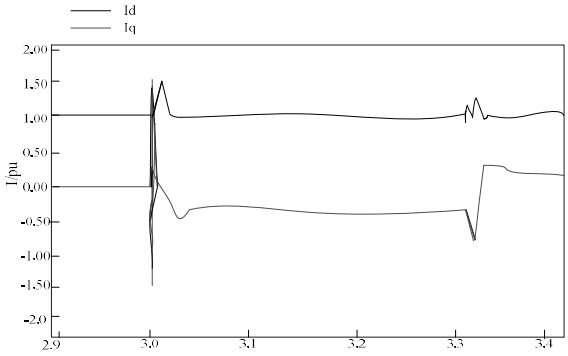

Figure 13. Active current and reactive current after control strategy

Figure 14 illustrates the system output effective power and passive power when the voltage drops by 30% after the system adopts the control strategy. The effective power drops to about 0.72 pu , and the passive power increment by about 0.33 pu .

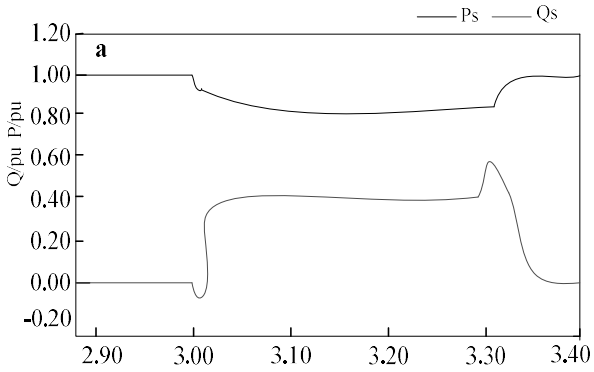

Figure 14: System output active power and reactive power

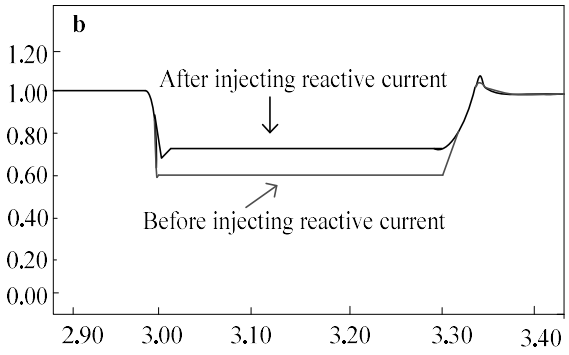

Figure 15: Comparison of grid-connected point voltage

Figure 15 illustrates the comparison of the grid-connected point voltage before and after the system adopts the control strategy. With the use of management measures, the grid-connected point voltage was increased from 0.68 pu to 0.72 pu .

IV. Discussion

In this simulation experiment, the low-volume crossing control measure was compared before and after application under two different voltage sag depths. In this simulation experiment, the low-volume crossing control measure

was compared before and after application under two different voltage sag depths. Experiments show that under the first drop depth test, the active power value without the reactive power support LVRT technology strategy is 0.314 pu higher than the reactive power support volume crossing control measure. In the second drop depth test, the reactive power value for which the reactive power support the low-volume crossing control measure is not adopted is 0. By adopting the reactive power support volume crossing control measure, after a certain amount of reactive power is transmitted through the grid, the reactive power of the grid-connected point is increased by 0.33pu. This means that when a PV shunt network fails due to varying degrees of voltage instability, the low-volume crossing control measure based on reactive current support proposed in this paper could be a useful solution to this situation. It can prevent over-current faults in PV plants, thereby achieving the low-volume crossing, and it can increase the grid-connected point volume to a certain extent.

V. Conclusion

The traditional energy development model once dominated. It has promoted social and economic development to a large extent, but traditional energy reserves are limited. With the continuous expansion of use, the remaining reserves are gradually becoming scarce, and the combustion of traditional energy sources has brought great harm to the environment, and the mode of replacing traditional energy generation with PV has attracted much attention. PV has become a hot spot for research and development by related scholars at this stage. PV can promote the simultaneous development of economic development and environmental protection. In-depth research on PV grid-connected systems is also an inevitable trend of energy development. Because of its characteristics, PV grid-connected systems are prone to voltage drops and failures when they are integrated into the power generation system. LVRT technology has a good effect on maintaining the stability of PV grid-connected point voltage.

This paper proposes a low-volume crossing control measure based on reactive power support, and the simulation experiment proves that this reactive power support is effective under different voltage drop depths. The LVRT control strategy is implemented on the basis of passive power support can guarantee that the PV inverter outputs current without overcurrent. When a failure occurs at the grid connection point, it can quickly provide a specific quantity of passive power support to the grid system within a short period of time. It can help the grid-connected point to recover from the fault caused by the voltage drop in time and realize the low-volume crossing. Through this control measure, it also helps enhance the electrical system reliability, showing its uniqueness and superiority that it does not have with other control strategies. Research on PV energy production equipment is still in progress. Although this article has made some achievements in the research of low-volume crossing control measure, there are still many shortcomings that need to be improved due to limited academic level and experimental conditions. The research scope of this paper is not enough. This paper only conducts the LVRT simulation experiment of reactive power support under the fault type of three-phase short circuit, without considering multiple types comprehensively. In the future research, it is necessary to carry out further research on the realization of LVRT control technology under various types of power generation system faults. Furthermore, the research depth of this article is not enough. In this paper, a low-volume crossing control simulation experiment is carried out for a three-phase grounded power grid fault. In the simulation experiment, during the voltage drop and recovery stage, the active current and the reactive current will generate a large number of shock waves. It takes some time to stabilize, which requires further optimization. The research of low-volume crossing control measure is complicated, but it also has great research value, and will continue to study in depth in future work.

References

[1] Haddadi A M, Farhangi S, Blaabjerg F. A Reliable Three-Phase Single-Stage Multiport Inverter for Grid-Connected Photovoltaic Applications. Emerging and Selected Topics in Power Electronics, IEEE Journal of, 2019, 7(4):2384-2393.

[2] Madeti S R, Singh S N. Online fault detection and the economic analysis of grid-connected photovoltaic systems. Energy, 2017, 134(sep.1):121-135.

[3] Zaim R, Jamaludin J, Rahim N A. Photovoltaic Flyback Microinverter With Tertiary Winding Current Sensing. IEEE Transactions on Power Electronics, 2019, 34(8):7588-7602.

[4] Hasanien H M. An Adaptive Control Strategy for Low Voltage Ride Through Capability Enhancement of Grid-Connected Photovoltaic Power Plants. IEEE Transactions on Power Systems, 2016, 31(4):3230-3237.

[5] Hassan Z, Amir A, Selvaraj J, et al. A review on current injection techniques for low-voltage ride-through and grid fault conditions in grid-connected photovoltaic system. Solar Energy, 2020, 207(47):851-873.

[6] Al-Shetwi A Q, Sujod M Z, Blaabjerg F, et al. Fault ride-through control of grid-connected photovoltaic power plants: A review. Solar Energy, 2019, 180(MAR.):340-350.

[7] Jaalam N, Rahim N A, Bakar A, et al. Strategy to enhance the low-voltage ride-through in photovoltaic system during multi-mode transition. Solar Energy, 2017, 153(sep.):744-754.

[8] Ntare R, Abbasy N H, Youssef K. Low Voltage Ride through Control Capability of a Large Grid Connected PV System Combining DC Chopper and Current Limiting Techniques. Journal of Power and Energy Engineering, 2019, 07(1):62-79.

[9] Shi K, Ye H, Xu P, et al. Low voltage ride through control strategy of virtual synchronous generator based on the analysis of excitation state. IET Generation Transmission & Distribution, 2018, 12(9):2165-2172.
[10] He Y, Wang M, Xu Z. Coordinative Low-Voltage-Ride-Through Control for the Wind-Photovoltaic Hybrid Generation System. IEEE Journal of Emerging and Selected Topics in Power Electronics, 2020, 8(2):1503-1514.
[11] Wang X, Liu S, Wang R, et al. Research on dynamic characteristics and stability of MMC photovoltaic grid-connected system based on rotational synchronous generator model. Electric power systems research, 2019, 173(AUG.):183-192.
[12] Al-Shamani A N, Sopian K, Mat S, et al. Performance enhancement of photovoltaic grid-connected system using PVT panels with nanofluid. Solar Energy, 2017, 150(jul.):38-48.
[13] Sahouane N, Dabou R, Ziane A, et al. Energy and economic efficiency performance assessment of a 28kWp photovoltaic grid-connected system under desertic weather conditions in Algerian Sahara. Renewable Energy, 2019, 143(DEC.):1318-1330.
[14] Wen H, Fazeli M. A low-voltage ride-through strategy using mixed potential function for three-phase grid-connected PV systems. Electric Power Systems Research, 2019, 173(AUG.):271-280.
[15] Dolu M K. Enhancement of Dynamic Modeling for LVRT Capability in DFIG-Based Wind Turbines. Iranian Journal of Science and Technology, Transactions of Electrical Engineering, 2020, 44(4):1345-1356.
[16] LOPEZ-SANTOS, Oswaldo, TILAGUY-LEZAMA, et al. Operation of a Photovoltaic Microinverter as Active Power Filter using the single phase P-Q Theory and Sliding Mode Control.. Ingeniería, 2017, 22(2):254-268.
[17] Fu G, Wang Y. Study of DQ frame control for PV grid-connected inverter. Energy education science and technology, 2016, 34(2):123-134.
[18] Lammert G, D Premm, Ospina L, et al. Control of Photovoltaic Systems for Enhanced Short-Term Voltage Stability and Recovery. IEEE Transactions on Energy Conversion, 2019, 34(1):243-254.
[19] Dolu M K. Enhancement of Dynamic Modeling for LVRT Capability in DFIG-Based Wind Turbines. Iranian Journal of Science and Technology, Transactions of Electrical Engineering, 2020, 44(4):1345-1356.
[20] Sadeghkhani I, Golshan M H, Mehrizi-Sani A, et al. Low-voltage ride-through of a droop-based three-phase four-wire grid-connected microgrid. IET Generation Transmission & Distribution, 2018, 12(8):1906–1914.
[21] Jianhua, Yuan, Yu, et al. Research on low-voltage ride through control based on model predictive control. The Journal of Engineering, 2017, 2017(13):2114-2118.
[22] Chen H C, Lee C T, Cheng P T, et al. A Low-Voltage Ride-Through Technique for Grid-Connected Converters With Reduced Power Transistors Stress. IEEE Transactions on Power Electronics, 2016, 31(12):8562-8571.
[23] Xing P, Fu L, Wang G, et al. A compositive control method of low-voltage ride through for PMSG-based wind turbine generator system. Iet Generation Transmission & Distribution, 2018, 12(1):117-125.
[24] Liu L, Geng H, Ma S, et al. Synchronization Stability and Reactive Current Control Method of DFIG Wind Farm During Low Voltage Ride Through. Proceedings of the CSEE, 2017, 37(15):4399-4407.
[25] Calle-Prado A, Alepuz S, Bordonau J, et al. Predictive Control of a Back-to-Back NPC Converter-Based Wind Power System. IEEE Transactions on Industrial Electronics, 2016, 63(7):4615-4627.